Proceedings of the Institution of Mechanical Engineers, Part G: Journal of Aerospace Engineering
http://pig.sagepub.com/

Non-linear flight control for unmanned aerial vehicles using adaptive backstepping based on invariant manifolds

Jiaming Zhang, Qing Li, Nong Cheng and Bin Liang

Proceedings of the Institution of Mechanical Engineers, Part G: Journal of Aerospace Engineering 2013 227: 33 originally published online 6 January 2012
DOI: 10.1177/0954410011430027

The online version of this article can be found at:
http://pig.sagepub.com/content/227/1/33

Published by:
SAGE
http://www.sagepublications.com

On behalf of:
Institution of Mechanical Engineers

Original Article

Institution of MECHANICAL ENGINEERS

Journal of AEROSPACE ENGINEERING

Proc IMechE Part G: J Aerospace Engineering
227(1) 33–44
© IMechE 2012
Reprints and permissions: sagepub.co.uk/journalsPermissions.nav
DOI: 10.1177/0954410011430027
uk.sagepub.com/jaero
SAGE

Non-linear flight control for unmanned aerial vehicles using adaptive backstepping based on invariant manifolds

Jiaming Zhang, Qing Li, Nong Cheng and Bin Liang

Abstract

A novel adaptive backstepping control scheme based on invariant manifolds for unmanned aerial vehicles in the presence of some uncertainties in the aerodynamic coefficients is presented in this article. This scheme is used for command tracking of the angle of attack, the sideslip angle, and the bank angle of the aircraft. The control law has a modular structure, which consists of a control module and a recently developed non-linear estimator. The estimator is based on invariant manifolds, which allows for prescribed dynamics to be assigned to the estimation error. The adaptive backstepping control law combined with the estimator covers the entire flight envelope and does not require accurate aerodynamic parameters. The stability of the whole closed-loop system is analyzed using the Lyapunov stability theory. The full six-degree-of-freedom non-linear model of a small unmanned aerial vehicle is used to demonstrate the effectiveness of the proposed control law. The numerical simulation result shows that this method can yield satisfying command tracking despite some unknown aerodynamic parameters.

Keywords

Flight control, backstepping, adaptive control, unmanned aerial vehicle

Date received: 11 May 2011; accepted: 26 October 2011

Introduction

Unmanned aerial vehicles (UAVs) are playing an increasingly important role in a large number of civilian and military applications and have received much interest in recent years. The primary objective of the flight control system design is to perform the stability augmentation and command augmentation for UAVs. Meanwhile, one important objective is to cut the cost of the flight control system. However, these objectives are often in conflict when using the classic flight control design approach. Traditionally, linear controllers are designed using the linearized aircraft model at many trimmed flight states.[1] These controllers are then combined using gain scheduling[2,3] as the function of flight states to guarantee the desired performance throughout the entire flight envelope. However, this process is tedious and costly. Furthermore, it does not give an optimal solution nor guarantee stability robustness.[4] Therefore, an advanced non-linear flight control law is required for the flight control system design.

One well-known non-linear design method is the feedback linearization, also called non-linear dynamic inversion.[5–7] In this approach, the original non-linear dynamic system is transformed into a linear system by coordinate transformation and state feedback.[8] However, one drawback of this method is that it requires an accurate aircraft mathematical model to perform perfect feedback linearization. It is generally not the case that an accurate mathematical model can be obtained because it is very difficult to precisely know the aerodynamic coefficients in the parameterized mathematical model. Additionally, this method is not economically preferable for UAVs. Therefore, to deal

Department of Automation, Tsinghua University, People's Republic of China

Corresponding author:
Jiaming Zhang, Department of Automation, Tsinghua University, Beijing 100084, People's Republic of China.
Email: zhangjm09@mails.tsinghua.edu.cn

with uncertainties, the adaptive feedback linearization[9–11] approach has been developed.

The flight control system based on the adaptive feedback linearization makes use of the two time-scale separation assumption that separates the fast dynamics from the slow dynamics. The inner and outer controllers corresponding to the fast and slow states are separately designed. The inherent drawback of this approach is that the gain of the inner controller needs to be large enough to insure that the transient dynamics of fast states is so quick that fast states have negligible effect on slow states. However, large gains of the inner controller may excite the high-frequency dynamics and cause the saturation of the actuator, even failing to guarantee the robustness of the stability.[12]

In response to these potential problems, the Lyapunov-based adaptive backstepping approach can be used to design the flight control system without assuming the two time-scale separation.[13–16] The adaptive backstepping method consists of a step-by-step coordinate transformation and designates some states as intermediate virtual control inputs to control other states. This method relies simultaneously on finding an adaptive control law and a parameter update law in order to cancel out the parameter-dependent terms of the derivative of the Lyapunov function, a quadratic function of the states, and the parameter estimation error, which guarantees that the Lyapunov function of the closed-loop system is negative. Therefore, all closed-loop signals are globally stable and bounded.

However, this method brings about a problem, in that the Lyapunov-based estimator only guarantees that the parameter estimation error is bounded and the estimate converges to an unknown constant value.[17] Thus, the modular backstepping approach has been proposed to overcome this problem. This approach consists of a controller and a separate estimator that is not Lyapunov-based, such as the neural networks[15] and the recursive least squares.[18] However, the dynamics of the estimation cannot be directly prescribed, which may lead to the undesired transient performance of the whole closed-loop system.

A new method which can be used to design the adaptive control law for uncertain non-linear systems based on immersion and invariance has been introduced in the study of Astolfi and Ortega,[19] see also the works of Astolfi et al.[20] and Karagiannis and Astolfi.[21] The detailed definition of immersion and invariance can be found in the works of Byrnes et al.[22] and Stephen.[23] This approach introduces a modular controller-estimator control scheme. The estimator allows for prescribing the dynamics of the parameter estimation error by driving the dynamics along invariant manifolds. In the study of Karagiannis and Astolfi,[24] the estimator based on invariant manifolds combined with an energy-based controller has been applied to UAV to achieve asymptotic command tracking in the presence of aerodynamic forces and moments with unknown coefficients based on the certainty equivalence principle. In the study of Sonneveldt et al.,[25] a command filtered backstepping law based on immersion and invariance with the addition of dynamic scaling factors and output filters has been applied to a simplified F-18 model. The adaptive control based on invariant manifolds has also been used in many other applications, such as the control system for the robot manipulator,[26] the aeroelastic system,[27] and the missile longitudinal autopilot.[28]

In this article, a novel adaptive flight control law based on invariant manifolds has been derived for a UAV. This method is neither based on two-time scale separation assumption nor the certainty equivalence principle. The objective of the fight control system is to follow the command of the angle of attack, the sideslip angle, and the bank angle. The aircraft model can be parameterized with some unknown coefficients. The control law consists of the estimator and the controller. The estimator based on invariant manifolds refers to the basic idea in the study of Karagiannis and Astolfi.[24] The backstepping control law combined with the estimator is introduced. The stability of the closed-loop system is guaranteed by the Lyapunov stability theory. The flight control law is applied to the full six-degree-of-freedom (6-DOF) non-linear aircraft model.

The outline of this article is organized as follows: First, the estimator based on invariant manifolds is briefly revisited and the adaptive backstepping control law is discussed in 'Adaptive control based on invariant manifolds' section. Then, the non-linear model of the aircraft is described in 'Aircraft dynamics' section. Thereafter, the specific flight control law for a small UAV is derived in 'Flight control system design' section. Finally, the performance of the adaptive flight control law is validated in 'Simulation' section via numerical simulations and conclusions are drawn in the last section.

Adaptive control based on invariant manifolds

Estimator based on invariant manifolds

The basic idea of the estimator based on invariant manifolds is briefly revisited in this section. This is a new approach to the design of the non-linear estimator for the uncertain non-linear system. This method relies upon the notion of the invariance of the manifold.

Consider the multivariable linearly parameterized system of the form

$$\dot{\boldsymbol{x}} = \boldsymbol{h}(\boldsymbol{x}, \boldsymbol{u}) + \boldsymbol{\Phi}^T(\boldsymbol{x})\boldsymbol{\theta} \tag{1}$$

with the state $\boldsymbol{x} \in R^n$ and input $\boldsymbol{u} \in R^m$, where $\boldsymbol{\theta} \in R^p$ is an unknown constant vector. Suppose that $\boldsymbol{\Phi}^T(\boldsymbol{x})\boldsymbol{\theta}$ is of the form

$$\boldsymbol{\Phi}^T(\boldsymbol{x})\boldsymbol{\theta} = \begin{bmatrix} \boldsymbol{\varphi}_1^T(x_1) & & 0 \\ & \ddots & \\ 0 & & \boldsymbol{\varphi}_n^T(x_n) \end{bmatrix} \begin{bmatrix} \boldsymbol{\theta}_1 \\ \vdots \\ \boldsymbol{\theta}_n \end{bmatrix} \tag{2}$$

with $\boldsymbol{\theta}_i \in R^{p_i}$ and $\sum_{i=1}^n p_i = p$. It should be noted that the uncertain parameterized non-linear dynamics is formulated in the form of the block diagonal matrix in which each block is treated as a function of the corresponding single-state variable to guarantee that the problem is solvable.

Unlike the traditional method, the estimator based on invariant manifolds provides an estimate of the unknown parameter, which is the sum of a partial estimate generated by an update law and a non-linear function. The estimator of the unknown vector is defined as

$$\hat{\boldsymbol{\theta}} = \xi + \boldsymbol{\eta} \tag{3}$$

where ξ is the partial estimate of the unknown parameter and $\boldsymbol{\eta}$ the chosen non-linear function. The dynamics of ξ is

$$\dot{\xi} = \boldsymbol{w} \tag{4}$$

where $\boldsymbol{w}$ is the update law to be determined later.

Define the manifold in the extended space (x, ξ)

$$M = \{(\boldsymbol{x}, \xi) \in R^2 \,|\, \xi + \boldsymbol{\eta} - \boldsymbol{\theta} = \boldsymbol{0}\} \tag{5}$$

The motivation behind this definition is that if the estimate is confined to the manifold, then the estimate $\hat{\boldsymbol{\theta}}$ reaches the true value $\boldsymbol{\theta}$. Therefore, the dynamics of the system combined with the estimator restricted to the manifold can be described by the equation

$$\dot{\boldsymbol{x}} = \boldsymbol{h}(\boldsymbol{x}, \boldsymbol{u}) + \boldsymbol{\Phi}^T(\boldsymbol{x})(\xi + \boldsymbol{\eta}) \tag{6}$$

if the manifold is invariant. Hence, the dynamics of the system is independent of the unknown parameter.

The following step is to ensure that the defined manifold M is attractive and invariant by selecting the proper update law and the non-linear function. Define the off-the-manifold co-ordinate $\boldsymbol{e} = \xi + \boldsymbol{\eta} - \boldsymbol{\theta}$, which also plays the role of an estimation error. Select the update law of ξ as follows

$$\boldsymbol{w} = -\frac{\partial \boldsymbol{\eta}}{\partial \boldsymbol{x}}[\boldsymbol{h} + \boldsymbol{\Phi}^T(\xi + \boldsymbol{\eta})] \tag{7}$$

Then, the dynamics of the estimation error behaves as

$$\dot{\boldsymbol{e}} = -\frac{\partial \boldsymbol{\eta}}{\partial \boldsymbol{x}}\boldsymbol{\Phi}^T\boldsymbol{e} \tag{8}$$

The selection of the update law $\boldsymbol{w}$ yields an equilibrium of zero, which guarantees that the manifold M is attractive. All that remains is to select the elements of the vector $\boldsymbol{\eta} = [\boldsymbol{\eta}_1, \boldsymbol{\eta}_2, \ldots, \boldsymbol{\eta}_n]^T$ so that the zero equilibrium of the system is also stable, which implies that the manifold is invariant. Referring to the study carried out by Karagiannis and Astolfi,[24] the non-linear function is chosen as

$$\boldsymbol{\eta}_i(x_i) = \gamma_i \int_0^{x_i} \boldsymbol{\varphi}_i(\lambda)\mathrm{d}\lambda \tag{9}$$

with $\gamma_i > 0$. Therefore, the dynamics of the estimation error is given as follows

$$\dot{\boldsymbol{e}} = -\boldsymbol{\Phi}(\boldsymbol{x})\boldsymbol{\Gamma}\boldsymbol{\Phi}^T(\boldsymbol{x})\boldsymbol{e} \tag{10}$$

where $\boldsymbol{\Gamma} = \mathrm{diag}(\gamma_1, \ldots, \gamma_n)$. The components of the estimation error vector satisfies

$$\dot{\boldsymbol{e}}_i = -\gamma_i\boldsymbol{\varphi}_i\boldsymbol{\varphi}_i^T\boldsymbol{e}_i \tag{11}$$

Therefore, the dynamics of the estimation error can be shaped by selecting the non-linear function. Then, increasing the gain γ_i can increase the speed of the estimation convergence. It should be noted that the block diagonal structure of the regressor matrix insures that the non-linear function can be determined.

The system (8) has a uniformly globally stable equilibrium at zero. Hence, the manifold M is attractive and invariant. Furthermore, $\boldsymbol{\Phi}(\boldsymbol{x})\boldsymbol{e}$ is square-integrable, i.e. $\boldsymbol{\Phi}(\boldsymbol{x}(t))\boldsymbol{e}(t) \in L_2$. It also implies that $\boldsymbol{\varphi}_i(x_i(t))^T\boldsymbol{e}_i(t) \in L_2$, $i = 1, 2, \ldots, n$. It follows from Barbalat's lemma that

$$\lim_{t\to\infty} \boldsymbol{\varphi}_i(x_i(t))^T\boldsymbol{e}_i(t) = 0 \tag{12}$$

Therefore, the estimate converges to the true value if components of the regressor are linearly independent, which can be easily satisfied.[24] Then, the estimator can be exploited by combining with the adaptive backstepping control law to regulate the cascaded system.

Adaptive backstepping

Consider the strict-feedback system of the form with uncertainties

$$\begin{aligned}\dot{x}_1 &= f_1(\bar{x}_1) + \boldsymbol{\varphi}_1(\bar{x}_1)^T\boldsymbol{\theta}_1 + g_1(\bar{x}_1)x_2\\ &\vdots\\ \dot{x}_i &= f_i(\bar{x}_i) + \boldsymbol{\varphi}_i(\bar{x}_i)^T\boldsymbol{\theta}_i + g_i(\bar{x}_i)x_{i+1}\\ &\vdots\\ \dot{x}_n &= f_n(\bar{x}_n) + \boldsymbol{\varphi}_n(\bar{x}_n)^T\boldsymbol{\theta}_n + g_n(\bar{x}_n)u\end{aligned} \tag{13}$$

with the state $x_i \in R$ and the control input u; $\bar{\boldsymbol{x}}_i = (x_1, x_2, \ldots, x_i)$; $\boldsymbol{\theta}_i$ is the vector of unknown constant parameters and $\boldsymbol{\varphi}_i(x)$ the known function vector, $i = 1, 2, \ldots, n$.

The control objective is to find a continuous adaptive state feedback control law so that the state x_1 tracks the smooth reference command $y_r(t)$. This class of systems can be stabilized using the adaptive backstepping.

The basic idea behind backstepping is to use some states as virtual controls to control other states. The backstepping design procedure starts by defining the tracking error as

$$z_i(t) = x_i - x_{i,r} \tag{14}$$

where $x_{i,r}$ is the intermediate desired control law to be designed. The dynamics of $z_i(t)$ can be written as

$$\begin{aligned}\dot{z}_1 &= f_1 + \boldsymbol{\varphi}_1^T\boldsymbol{\theta}_1 + g_1 z_2 + g_1 x_{2,r} - \dot{x}_{1,r}\\ &\vdots\\ \dot{z}_i &= f_i + \boldsymbol{\varphi}_i^T\boldsymbol{\theta}_i + g_i z_{i+1} + g_i x_{i+1,r} - \dot{x}_{i,r}\\ &\vdots\\ \dot{z}_n &= f_n + \boldsymbol{\varphi}_n^T\boldsymbol{\theta}_n + g_n u - \dot{x}_{n,r}\end{aligned} \tag{15}$$

The virtual controls are proposed as follows

$$x_{i+1,r} = -g_i^{-1}[f_i + \boldsymbol{\varphi}_i^T(\xi_i + \boldsymbol{\eta}_i) + g_{i-1}z_i + k_i z_i - \dot{x}_{i,r}] \tag{16}$$

with $i = 1, 2, \ldots, n-1$, $k_i > 1$, and $g_0 = 0$. In the last design step, the real control is determined as

$$u = -g_n^{-1}[f_n + \boldsymbol{\varphi}_n^T(\xi_n + \boldsymbol{\eta}_n) + g_{n-1}z_n + k_n z_n - \dot{x}_{n,r}] \tag{17}$$

with $k_n > 1$.

For the stability analysis of the closed-loop system, consider the following Lyapunov function

$$V_c = \sum_{i=1}^{n}\left(z_i^T z_i + \frac{1}{\gamma_i}\boldsymbol{e}_i^T\boldsymbol{e}_i\right) \tag{18}$$

Taking the time derivative of V_c and using equations (8), (10), and (11) yield

$$\begin{aligned}\dot{V}_c &= 2\sum_{i=1}^{n-1} z_i^T(f_i + \boldsymbol{\varphi}_i^T\boldsymbol{\theta}_i + g_i z_{i+1} + g_i x_{i+1,r} - \dot{x}_{i,r})\\ &\quad + 2z_n^T(f_n + \boldsymbol{\varphi}_n^T\boldsymbol{\theta}_n + g_n u - \dot{x}_{n,r}) - 2\sum_{i=1}^{n}\|\boldsymbol{\varphi}_i^T\boldsymbol{e}_i\|^2\\ &= -2\sum_{i=1}^{n-1} z_i^T(k_i z_i + \boldsymbol{\varphi}_i^T\boldsymbol{e}_i - g_i z_{i+1} + g_{i-1}z_i)\\ &\quad - 2z_n^T(k_n z_n + \boldsymbol{\varphi}_n^T\boldsymbol{e}_n + g_{n-1}z_n) - 2\sum_{i=1}^{n}\|\boldsymbol{\varphi}_i^T\boldsymbol{e}_i\|^2\\ &= -2\sum_{i=1}^{n} k_i\|z_i\|^2 - 2\sum_{i=1}^{n} z_i^T\boldsymbol{\varphi}_i^T\boldsymbol{e}_i - 2\sum_{i=1}^{n}\|\boldsymbol{\varphi}_i^T\boldsymbol{e}_i\|^2\end{aligned}$$

Using Yong's inequality

$$\|z_i^T\boldsymbol{\varphi}_i^T\boldsymbol{e}_i\| \leqslant \frac{\|z_i\|^2 + \|\boldsymbol{\varphi}_i^T\boldsymbol{e}_i\|^2}{2} \tag{19}$$

the Lyapunov function satisfies

$$\dot{V}_c \leqslant -\sum_{i=1}^{n} 2(k_i - 1)\|z_i\|^2 - \sum_{i=1}^{n}\|\boldsymbol{\varphi}_i^T\boldsymbol{e}_i\|^2$$

If $k_i > 1$, the derivative of the Lyapunov function V_c is negative definite. It can be concluded that the closed-loop system of equation (15) has a globally stable equilibrium of zero and $\lim_{t\to\infty} x_i = x_{i,r}$ using Barbalat's lemma. It should be noted that this method does not depend on canceling out the parameter-dependent terms of the derivative of the Lyapunov function, unlike the classical adaptive control law. Thereby, the adaptive backstepping control law based on invariant manifolds can be applied for the flight control system design to track the reference command.

Aircraft dynamics

In this study, the aircraft is a small UAV which was developed by ETH Zurich.[29] The aircraft is equipped with five control surfaces, i.e. the left aileron, the right aileron, the left elevator, the right elevator, and the rudder, each of which is fully independent.

Based on the assumption of the flat Earth and the constant mass, the full 6-DOF non-linear equations of a rigid-body aircraft are given as follows.[30]

Force equations

$$\begin{aligned}\dot{V}_T &= \frac{1}{m}(X + F_T\cos\alpha\cos\beta + mg_1)\\ \dot{\alpha} &= q - (p\cos\alpha + r\sin\alpha)\tan\beta\\ &\quad + \frac{1}{mV_T\cos\beta}(Z - F_T\sin\alpha + mg_3)\\ \dot{\beta} &= p\sin\alpha - r\cos\alpha +\\ &\quad \frac{1}{mV_T}(Y - F_T\cos\alpha\sin\beta + mg_2)\end{aligned} \tag{20}$$

Kinematic equations

$$\begin{aligned}\dot{\phi} &= p + \tan\theta(q\sin\phi + r\cos\phi)\\ \dot{\theta} &= q\cos\phi - r\sin\phi\\ \dot{\psi} &= \frac{q\sin\phi + r\cos\phi}{\cos\theta}\end{aligned} \tag{21}$$

Moment equations

$$\begin{aligned}\dot{p} &= (c_1 r + c_2 p)q + c_3 L + c_4 N\\ \dot{q} &= c_5 pr - c_6(p^2 - r^2) + c_7 M\\ \dot{r} &= (c_8 p - c_2 r)q + c_4 L + c_9 N\end{aligned} \tag{22}$$

where V_t is the airspeed, α the angle of attack, and β the sideslip angle; $\begin{bmatrix}\phi & \theta & \psi\end{bmatrix}^T$ represent the standard Euler angles: roll, pitch, and yaw; $\begin{bmatrix}p & q & r\end{bmatrix}^T$ are the body fixed rotational angular rates; m is the mass; $\begin{bmatrix}X & Y & Z\end{bmatrix}^T$ are the aerodynamic forces: drag, lateral, and lift force; F_T represents the thrust which is produced by the propeller and it is assumed that the thrust is through the center of gravity of the aircraft; $\begin{bmatrix}L & M & N\end{bmatrix}^T$ are the aerodynamic moments: the roll, pitch, and yaw moments. The components of the gravity vector are given by

$$\begin{aligned}g_1 &= g(-\cos\alpha\cos\beta\sin\theta + \sin\beta\sin\phi\cos\theta\\ &\quad + \sin\alpha\cos\beta\cos\phi\cos\theta)\\ g_2 &= g(\cos\alpha\sin\beta\sin\theta + \cos\beta\sin\phi\cos\theta\\ &\quad - \sin\alpha\sin\beta\cos\phi\cos\theta)\\ g_3 &= g(\sin\alpha\sin\theta + \cos\alpha\cos\phi\cos\theta)\end{aligned} \tag{23}$$

where g is the gravitational constant. The moments of inertia are defined as follows

$$\begin{aligned}&\Gamma c_1 = (I_y - I_z)I_z - I_{xz}^2 \quad \Gamma c_2 = (I_x - I_y + I_z)I_{xz}\\ &\Gamma c_3 = I_z \quad \Gamma c_4 = I_{xz} \quad c_5 = \frac{I_z - I_x}{I_y} \quad c_6 = \frac{I_{xz}}{I_y}\\ &c_7 = \frac{1}{I_y} \quad \Gamma c_8 = I_x(I_x - I_y) + I_{xz}^2 \quad \Gamma c_9 = I_x\end{aligned}$$

with $\Gamma = I_x I_z - I_{xz}^2$.

It should be noted that force equations of the aircraft are expressed in the wind-axes and the kinematic and moment equations in the body-axes. In this article, the pitch angle is under the constraint $-\pi/2 < \theta < \pi/2$, or else the aircraft non-linear dynamics can be computed with the quaternion representation.[30]

The aerodynamic forces are defined as the function of the angle of attack and the sideslip angle

$$\begin{aligned}X &= \bar{q}\,S(C_{X1} + C_{X\alpha}\alpha + C_{X\alpha 2}\alpha^2 + C_{X\beta 2}\beta^2)\\ Y &= \bar{q}\,SC_{Y\beta}\beta\\ Z &= \bar{q}\,S(C_{Z1} + C_{Z\alpha}\alpha)\end{aligned} \tag{24}$$

where $\bar{q} = \rho V_T^2/2$ is the dynamic pressure, ρ the air density which is computed according to the International Standard Atmosphere model, S and the reference wing area. To verify the adaptive control law, the stability derivatives $C_{Y\beta}$ and $C_{Z\alpha}$ are assumed to be unknown coefficients; the dimensionless coefficient C_{Z1} is assumed to be known because it is trivial compared with the stability derivatives. It should be noted that the control surface deflections have no effect on the aerodynamic force components, which is a general assumption in the studies of Shin and Kim[12] and Li et al.[16]

The aerodynamic moments are modeled as[29]

$$\begin{aligned}L &= \bar{q}\,Sb(C_{L1}\delta_{a1} + C_{L2}\delta_{a2} + C_{L3}\delta_{e1} + C_{L4}\delta_{e2}\\ &\quad + C_{L\beta}\beta + C_{Lp}\tilde{p} + C_{Lr}\tilde{r})\\ M &= \bar{q}\,S\bar{c}(C_{M1}\delta_{a1} + C_{M2}\delta_{a2} + C_{M3}\delta_{e1}\\ &\quad + C_{M4}\delta_{e2} + C_{Mq}\tilde{q} + C_{M\alpha}\alpha)\\ N &= \bar{q}\,Sb(C_{N\delta_r}\delta_r + C_{Nr}\tilde{r} + C_{N\beta}\beta)\end{aligned} \tag{25}$$

where b is the reference wing span, $\bar{c}$ the reference mean aerodynamic chord, δ_{a1} and δ_{a2} the left and right aileron deflections, δ_{e1} and δ_{e2} the left and right elevator deflections, and δ_r the rudder deflection. The dimensionless angular rates are introduced as

$$\tilde{p} = \frac{bp}{2V_T}, \quad \tilde{q} = \frac{\bar{c}\,q}{2V_T}, \quad \tilde{r} = \frac{br}{2V_T} \tag{26}$$

The control effectiveness coefficients C_{L1}, C_{L2}, C_{L3}, C_{L4}, C_{M1}, C_{M2}, C_{M3}, C_{M4}, and $C_{N\delta_r}$ are assumed to be known to insure that the adaptive control problem is solvable similar to that of Karagiannis and Astolfi.[24] The damping factors C_{Lp}, C_{Nr}, and C_{Mq} are assumed to be unknown parameters. $C_{L\beta}$, C_{Lr}, $C_{M\alpha}$, and $C_{N\beta}$ are trivial compared with the damping factors. Furthermore, α and β are expressed in radian and usually small. Therefore, for simplicity, it is reasonable to assume these factors to be known, taking into account the limited computational capacity of the aircraft.

The convention used here for ailerons and elevators is positive deflection when the control surface is up and negative deflection when the control surface is down. For the rudder, positive deflection occurs when the rudder deflects to the right. The five control surfaces of the aircraft can be separately driven by actuators to produce the deflections commanded by the flight control system. This provides the control redundancy considering the fault circumstance; however, this is not the focus of this article. The actuators of the control surfaces are modeled as first-order low-pass filters with time constant $\tau = 0.05\,\mathrm{s}$. The saturation limits of the actuators are $\pm 45^\circ$.[31]

The thrust force F_T is generated by the propeller

$$F_T = \rho n^2 D^4 C_{FT} \tag{27}$$

where n represents the speed of the engine, which is modeled as a first-order low-pass filter with the time constant $\tau_n = 0.4\,\mathrm{s}$, D the diameter of the propeller, and C_{FT} the dimensionless thrust coefficient.[29]

Flight control system design

In this section, an adaptive flight control system is constructed based on the proposed method in 'Adaptive control based on invariant manifolds' section in order to track the smooth reference commands ϕ_d, α_d, and β_d. The framework of the flight control system is shown in Figure 1. The flight control system has a modular structure and the designs of the control module and the estimator are separately performed.

Estimator design

Since there are some unknown aerodynamic force and moment coefficients in the aircraft dynamics, estimators based on invariant manifolds for the unknown aerodynamic force and moment coefficients are individually designed. If one defines the state $\boldsymbol{x}_1 = \begin{bmatrix} x_{11} & x_{12} & x_{13} \end{bmatrix}^T = \begin{bmatrix} \phi & \alpha & \beta \end{bmatrix}^T$, the non-linear dynamics of the aircraft can be rewritten as

$$\dot{\boldsymbol{x}}_1 = \boldsymbol{h}(\boldsymbol{x}_1) + \boldsymbol{\Phi}(\boldsymbol{x}_1)^T \boldsymbol{\theta} \tag{28}$$

The elements of $\boldsymbol{h}(\boldsymbol{x}_1) = [\,h_1 \quad h_2 \quad h_3\,]^T$ are

$$\begin{aligned}
h_1 &= p + \tan\theta(q\sin\phi + r\cos\phi)\\
h_2 &= q - (p\cos\alpha + r\sin\alpha)\tan\beta\\
&\quad + \frac{1}{mV_T\cos\beta}(\bar{q}\,SC_{Z1} - F_T\sin\alpha + mg_3)\\
h_3 &= p\sin\alpha - r\cos\alpha\\
&\quad + \frac{1}{mV_T}(-F_T\cos\alpha\sin\beta + mg_2)
\end{aligned} \tag{29}$$

The elements of $\boldsymbol{\Phi}(\boldsymbol{x}_1) = \mathrm{diag}(\,\boldsymbol{\varphi}_1 \quad \boldsymbol{\varphi}_2 \quad \boldsymbol{\varphi}_3\,)$ are

$$\begin{aligned}
\boldsymbol{\varphi}_1 &= 0\\
\boldsymbol{\varphi}_2 &= \frac{1}{mV_T\cos\beta}\bar{q}\,S\alpha\\
\boldsymbol{\varphi}_3 &= \frac{1}{mV_T}\bar{q}\,S\beta
\end{aligned} \tag{30}$$

The elements of the unknown parameter vector $\boldsymbol{\theta}$ are $\theta_1 = 0$, $\theta_2 = C_{Z\alpha}$, and $\theta_3 = C_{Y\beta}$. It should be noted that the equation of the bank angle ϕ depicts the kinematic relation. Therefore, no unknown parameters exist and the terms accordingly $\boldsymbol{\varphi}_1$ and θ_1 are treated as zero. To construct the estimator, the update law of $\boldsymbol{\xi} = [\,\xi_1 \quad \xi_2 \quad \xi_3\,]^T$ is determined as

$$\dot{\xi}_i = -\frac{\partial\eta_i}{\partial x_{1i}}[h_i + \boldsymbol{\varphi}_i^T(\xi_i + \eta_i)] \tag{31}$$

$i = 1, 2, 3$. According to equation (9), the components of the non-linear function $\boldsymbol{\eta} = [\,\eta_1 \quad \eta_2 \quad \eta_3\,]^T$ are selected as

$$\begin{aligned}
\eta_1 &= 0\\
\eta_2 &= \frac{\gamma_2}{2mV_T\cos\beta}\bar{q}\,S\alpha^2\\
\eta_3 &= \frac{\gamma_3}{2mV_T}\bar{q}\,S\beta^2
\end{aligned} \tag{32}$$

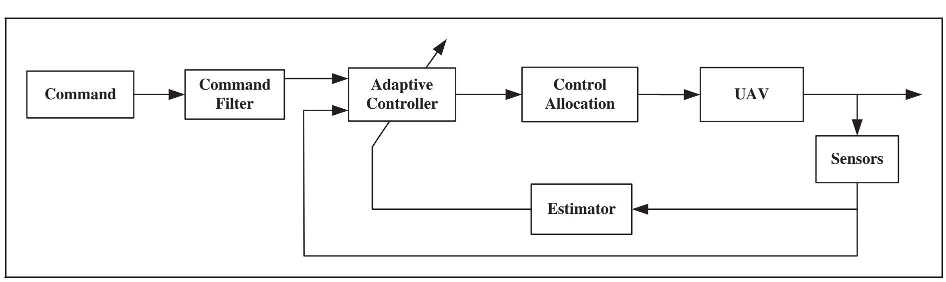

Figure 1. Framework of the flight control system.

Note that the non-linear function η_1 corresponding to $\boldsymbol{\varphi}_1$ is selected as zero. The estimate $\hat{\theta}_i$ of the unknown parameter θ_i is the sum of ξ_i and η_i, $i=1, 2, 3$.

Next, the following step is to design the estimator for unknown parameters of the aerodynamic moment. Defining the state $\boldsymbol{x}_2 = \begin{bmatrix} x_{21} & x_{22} & x_{23}\end{bmatrix}^T = \begin{bmatrix} p & q & r\end{bmatrix}^T$, the moment equations can be written as

$$\dot{x}_2 = \boldsymbol{h}'(\boldsymbol{x}_2) + \boldsymbol{\Phi}'(\boldsymbol{x}_2)^T\boldsymbol{\theta}' \tag{33}$$

The elements of $\boldsymbol{h}'(\boldsymbol{x}_2) = [\,h'_1 \quad h'_2 \quad h'_3\,]^T$ are

$$\begin{aligned} h'_1 &= (c_1 r + c_2 p)q + c_3\bar{q}Sb(C_{L1}\delta_{a1} + C_{L2}\delta_{a2} + C_{L3}\delta_{e1} \\ &\quad + C_{L4}\delta_{e2} + C_{L\beta}\beta + C_{Lr}\tilde{r}) + c_4\bar{q}Sb(C_{N\delta_r}\delta_r + C_{N\beta}\beta) \\ h'_2 &= c_5 pr - c_6(p^2 - r^2) + c_7\bar{q}S\bar{c}(C_{M1}\delta_{a1} + C_{M2}\delta_{a2} \\ &\quad + C_{M3}\delta_{e1} + C_{M4}\delta_{e2} + C_{M\alpha}\alpha) \\ h'_3 &= (c_8 p - c_2 r)q + c_4\bar{q}Sb(C_{L1}\delta_{a1} + C_{L2}\delta_{a2} + C_{L3}\delta_{e1} \\ &\quad + C_{L4}\delta_{e2} + C_{L\beta}\beta + C_{lr}\tilde{r}) + C_9\bar{q}Sb(C_{N\delta_r}\delta_r + C_{N\beta}\beta) \end{aligned} \tag{34}$$

The elements of $\boldsymbol{\Phi}'(\boldsymbol{x}_2)$ are

$$\begin{aligned} \boldsymbol{\varphi}'_1 &= \bar{q}\,Sb[\,c_3\,\tilde{p} \quad c_4\,\tilde{r}\,]^T \\ \boldsymbol{\varphi}'_2 &= c_7\,\bar{q}\,S\,\bar{c}\,\tilde{q} \\ \boldsymbol{\varphi}'_3 &= \bar{q}\,Sb[\,c_4\,\tilde{p} \quad c_9\,\tilde{r}\,]^T \end{aligned} \tag{35}$$

The components of the unknown parameter $\boldsymbol{\theta}'$ are $\theta'_1 = [\,C_{Lp} \quad C_{Nr}\,]^T$, $\theta'_2 = C_{Mq}$, and $\theta'_3 = [\,C_{Lp} \quad C_{Nr}\,]^T$. Then, the update law of $\xi' = [\,\xi'_1 \quad \xi'_2 \quad \xi'_3\,]^T$ is determined as

$$\dot{\xi}'_i = -\frac{\partial\eta'_i}{\partial x_{2i}}[h'_i + \boldsymbol{\varphi}'^T_i(\xi'_i + \eta'_i)] \tag{36}$$

$i=1, 2, 3$. According to equation (9), selecting the components of the non-linear function $\boldsymbol{\eta}' = [\,\eta'_1 \quad \eta'_2 \quad \eta'_3\,]^T$

$$\begin{aligned} \eta'_1 &= \gamma'_1\,\bar{q}\,Sb\left[\frac{1}{2}c_3\,\tilde{p}\,p \quad c_4\,\tilde{r}\,p\right]^T \\ \eta'_2 &= \frac{1}{2}\gamma'_2\,\bar{q}\,S\,\bar{c}\,\tilde{q}\,q \\ \eta'_3 &= \gamma'_3\,\bar{q}\,Sb\left[c_4\,\tilde{p}\,r \quad \frac{1}{2}c_9\,\tilde{r}\,r\right]^T \end{aligned} \tag{37}$$

The estimate $\hat{\theta}'_i$ of the unknown parameter θ'_i is the sum of ξ'_i and η'_i, $i=1, 2, 3$. It should be noted that the dynamics of the roll and yaw rates are coupled and contain same unknown roll and yaw moment parameters. Therefore, θ'_1 is identical to θ'_3, which guarantees the block diagonal structure of the regressor matrix. However, they are separately identified by different specific estimators.

Adaptive control law

The adaptive backstepping control law discussed in 'Adaptive control based on invariant manifolds' section can be stated in a multivariable form. Defining the control $\boldsymbol{u} = \begin{bmatrix}\delta_{a1} & \delta_{a2} & \delta_{e1} & \delta_{e2} & \delta_r\end{bmatrix}^T$, the dynamics of the aircraft can be rewritten in a vector form

$$\begin{aligned} \dot{\boldsymbol{x}}_1 &= \boldsymbol{f}_1(\boldsymbol{x}_1) + \boldsymbol{\Phi}_1(\boldsymbol{x}_1)^T\boldsymbol{\theta}_1 + \boldsymbol{g}_1(\boldsymbol{x}_1)\boldsymbol{x}_2 \\ \dot{\boldsymbol{x}}_2 &= \boldsymbol{f}_2(\boldsymbol{x}_1, \boldsymbol{x}_2) + \boldsymbol{\Phi}_2(\boldsymbol{x}_1, \boldsymbol{x}_2)^T\boldsymbol{\theta}_2 + \boldsymbol{g}_2(\boldsymbol{x}_1, \boldsymbol{x}_2)\boldsymbol{u} \end{aligned} \tag{38}$$

The components of $\boldsymbol{f}_1(\boldsymbol{x}_1)$ are given by

$$\begin{aligned} f_\phi &= 0 \\ f_\alpha &= \frac{1}{mV_T\cos\beta}(\bar{q}\,SC_{Z1} - F_T\sin\alpha + mg_3) \\ f_\beta &= \frac{1}{mV_T}(-F_T\cos\alpha\sin\beta + mg_2) \end{aligned} \tag{39}$$

The term $\boldsymbol{g}_1(\boldsymbol{x}_1)$ is

$$\boldsymbol{g}_1 = \begin{bmatrix} 1 & \tan\theta\sin\phi & \tan\theta\cos\phi \\ -\cos\alpha\tan\beta & 1 & -\sin\alpha\tan\beta \\ \sin\alpha & 0 & -\cos\alpha \end{bmatrix} \tag{40}$$

Now, the matrix $\boldsymbol{g}_1(\boldsymbol{x}_1)$ describes the kinematic relationship and is identical for any aircraft. It can be proven that $\boldsymbol{g}_1(\boldsymbol{x}_1)$ is invertible for all ϕ and the reasonable ranges of α, β, and θ.[32] The components of $\boldsymbol{f}_2(x_1, x_2)$ are

$$\begin{aligned} f_p &= (c_1 r + c_2 p)q + c_3\,\bar{q}\,Sb(C_{L\beta}\beta + C_{Lr}\,\tilde{r}) \\ &\quad + c_4\,\bar{q}\,SbC_{N\beta}\beta \end{aligned} \tag{41}$$

$$f_q = c_5 pr - c_6(p^2 - r^2) + c_7\,\bar{q}\,S\,\bar{c}\,C_{M\alpha}\alpha \tag{42}$$

$$\begin{aligned} f_r &= (c_8 p - c_2 r)q + c_4\,\bar{q}\,Sb(C_{L\beta}\beta + C_{Lr}\,\tilde{r}) \\ &\quad + c_9\,\bar{q}\,SbC_{N\beta}\beta \end{aligned} \tag{43}$$

The term $\boldsymbol{g}_2$ is

$$\boldsymbol{g}_2 = \bar{q}\,S\begin{bmatrix} c_3bC_{L1} & c_3bC_{L2} & c_3bC_{L3} & c_3bC_{L4} & c_4bC_{N\delta_r} \\ c_7\,\bar{c}\,C_{M1} & c_7\,\bar{c}\,C_{M2} & c_7\,\bar{c}\,C_{M3} & c_7\,\bar{c}\,C_{M4} & 0 \\ c_4bC_{L1} & c_4bC_{L2} & c_4bC_{L3} & c_4bC_{L4} & c_9bC_{N\delta_r} \end{bmatrix} \tag{44}$$

The control objective is to track the reference $\boldsymbol{x}_{1,r} = \begin{bmatrix} \phi_d & \alpha_d & \beta_d \end{bmatrix}^T$. The design procedure is initiated by defining the tracking errors as

$$\begin{bmatrix} z_{11} \\ z_{12} \\ z_{13} \end{bmatrix} = \begin{bmatrix} \phi - \phi_d \\ \alpha - \alpha_d \\ \beta - \beta_d \end{bmatrix} \tag{45}$$

and

$$\begin{bmatrix} z_{21} \\ z_{22} \\ z_{23} \end{bmatrix} = \begin{bmatrix} p - p_d \\ q - q_d \\ r - r_d \end{bmatrix} \tag{46}$$

where p_d, q_d, and r_d are the virtual control commands. Using the adaptive backstepping method, the virtual commands are determined as

$$\begin{bmatrix} p_d \\ q_d \\ r_d \end{bmatrix} = -\boldsymbol{g}_1^{-1} \left(\begin{bmatrix} f_\phi + \boldsymbol{\varphi}_1^T \hat{\theta}_1 \\ f_\alpha + \boldsymbol{\varphi}_2^T \hat{\theta}_2 \\ f_\beta + \boldsymbol{\varphi}_3^T \hat{\theta}_3 \end{bmatrix} + \begin{bmatrix} k_1 z_{11} \\ k_2 z_{12} \\ k_3 z_{13} \end{bmatrix} - \begin{bmatrix} \dot{\phi}_d \\ \dot{\alpha}_d \\ \dot{\beta}_d \end{bmatrix} \right) \tag{47}$$

The unknown parameter θ_i is replaced by its corresponding estimate $\hat{\theta}_i$ which is the sum of ξ_i and η_i, $i = 1, 2, 3$. The surface deflections are determined as

$$\begin{bmatrix} \delta_{a1} \\ \delta_{a2} \\ \delta_{e1} \\ \delta_{e2} \\ \delta_r \end{bmatrix} = -\boldsymbol{g}_2^{+} \left(\begin{bmatrix} f_p + \boldsymbol{\varphi}_1' T \hat{\theta}_1' \\ f_q + \boldsymbol{\varphi}_2' T \hat{\theta}_2' \\ f_r + \boldsymbol{\varphi}_3' T \hat{\theta}_3' \end{bmatrix} + \boldsymbol{g}_1 \begin{bmatrix} z_{21} \\ z_{22} \\ z_{23} \end{bmatrix} + \begin{bmatrix} k_1' z_{21} \\ k_2' z_{22} \\ k_3' z_{23} \end{bmatrix} - \begin{bmatrix} \dot{p}_d \\ \dot{q}_d \\ \dot{r}_d \end{bmatrix} \right) \tag{48}$$

Generally, $\boldsymbol{g}_2(x_2)$ is of rank 3, and therefore $\boldsymbol{g}_2^{+}(\boldsymbol{x}_2)$ represents the pseudo-inverse[33] of $\boldsymbol{g}_2(x_2)$ used to distribute the desired control signals over the actual inputs. The unknown parameter θ_i' is replaced by its corresponding estimate $\hat{\theta}_i'$. Finally, note that the thrust is controlled to maintain the constant airspeed referring to the method proposed in the study of Ducard and Geering,[34] which is not presented here.

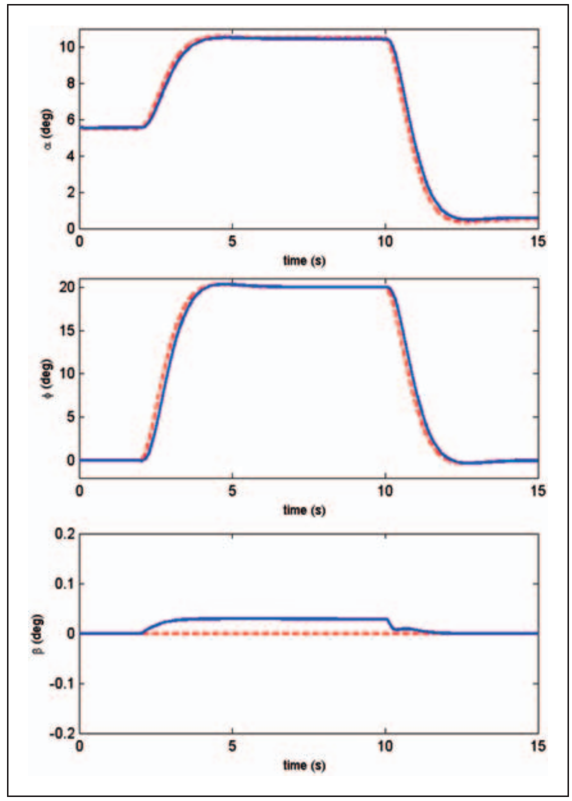

Figure 2. Reference commands tracking.

Simulations

This section presents the simulation results from the application of the proposed adaptive control law to the full 6-DOF model of a small UAV. Both the control law and the aircraft model are implemented in an MATLAB/Simulink environment. The detailed data of the non-linear model, such as the aircraft geometry and the aerodynamic coefficients, can be obtained from the study of Ducard and Geering.[29] The purpose of the simulation is to verify the convergence performance of the estimation algorithm and the tracking performance of the control algorithm. Therefore, some aerodynamic coefficients are assumed to be unknown as stated in 'Aircraft dynamics'. The simulation starts from a steady-level flight at an altitude 500 m and an initial velocity 30 m/s.

In this simulation, it is required that the angle of attack and the bank angle must follow the reference signals. Meanwhile, the sideslip angle is always kept at zero. The commands are given as follows

$$\begin{cases} \alpha_c = 5.4^\circ, & \phi_c = 0^\circ, & \beta_c = 0^\circ, & 0 \leqslant t \leqslant 2s \\ \alpha_c = 10^\circ, & \phi_c = 20^\circ, & \beta_c = 0^\circ, & 2 \leqslant t \leqslant 10s \\ \alpha_c = 0^\circ, & \phi_c = 0^\circ, & \beta_c = 0^\circ, & 10 \leqslant t \leqslant 15s \end{cases}$$

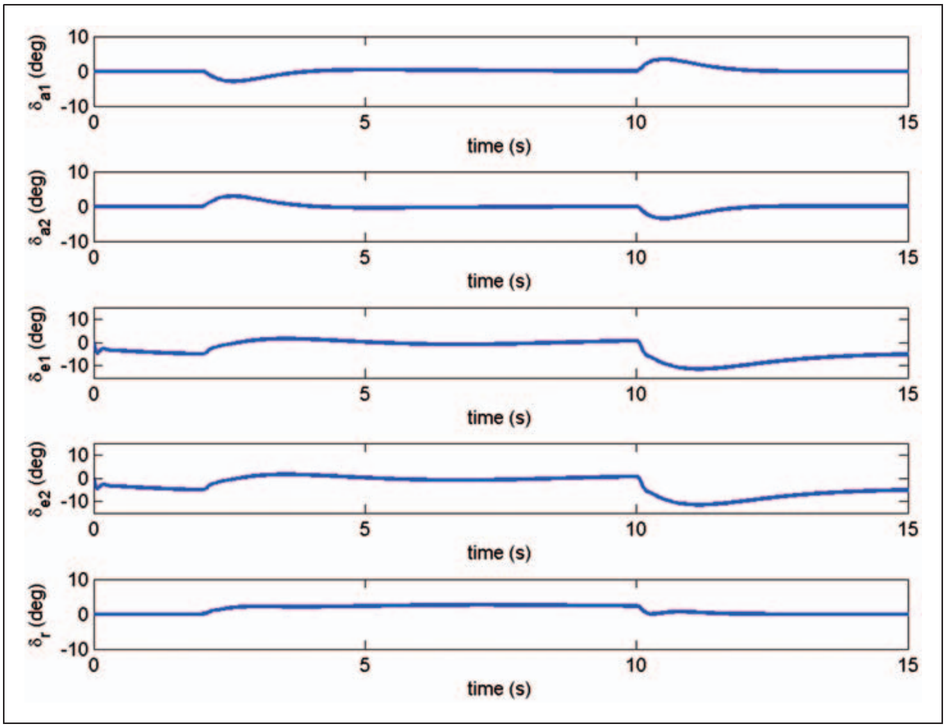

Figure 3. Time histories of control surface deflections.

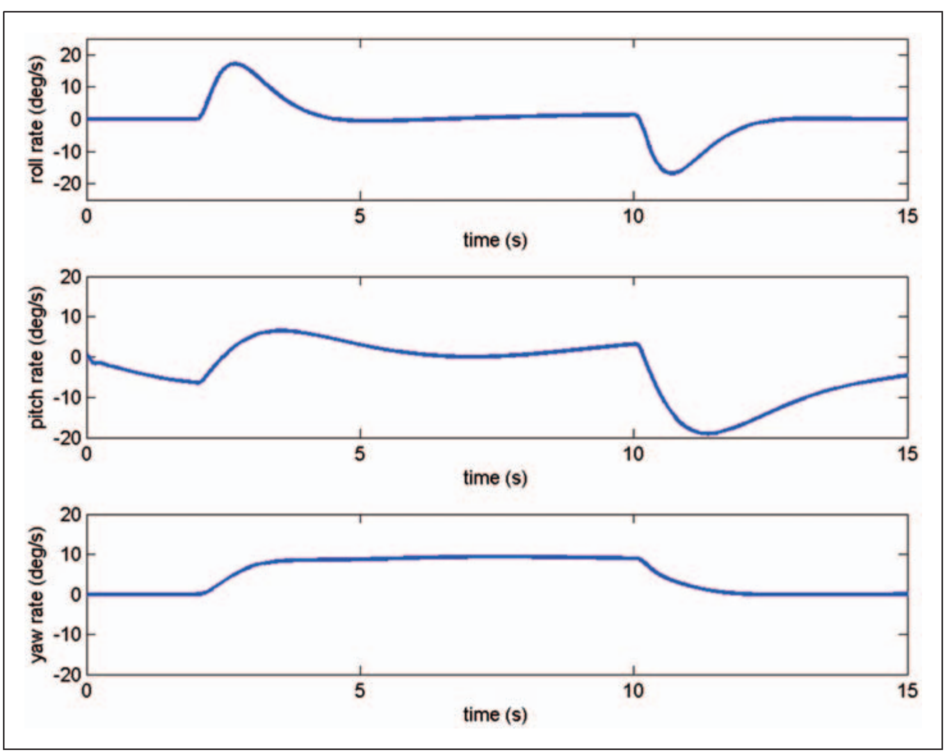

Figure 4. Time histories of angular rates.

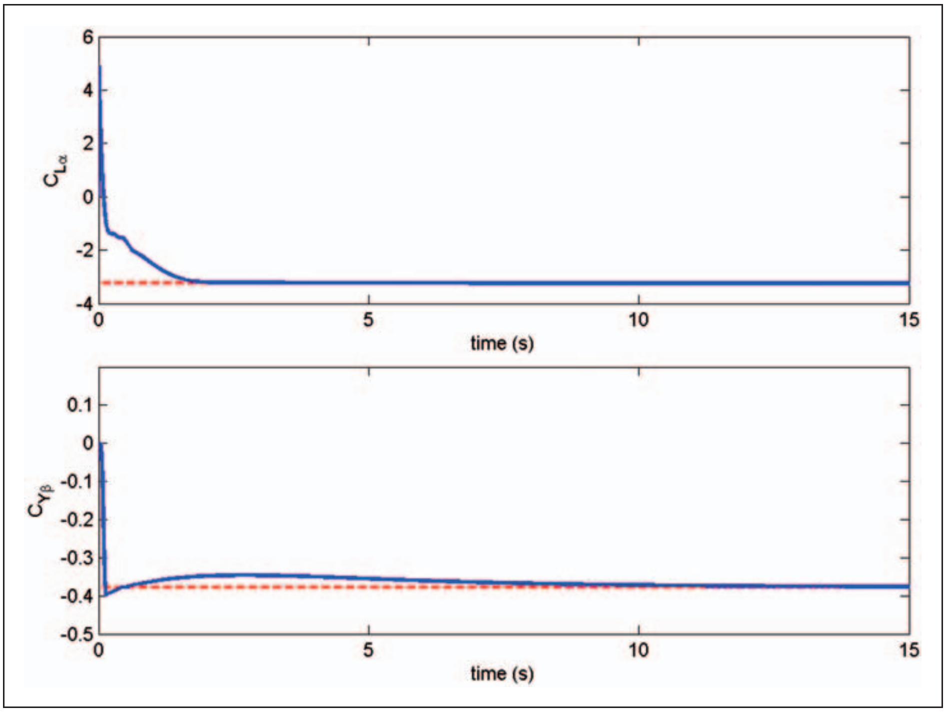

Figure 5. Time histories of the estimation for the aerodynamic force coefficients.

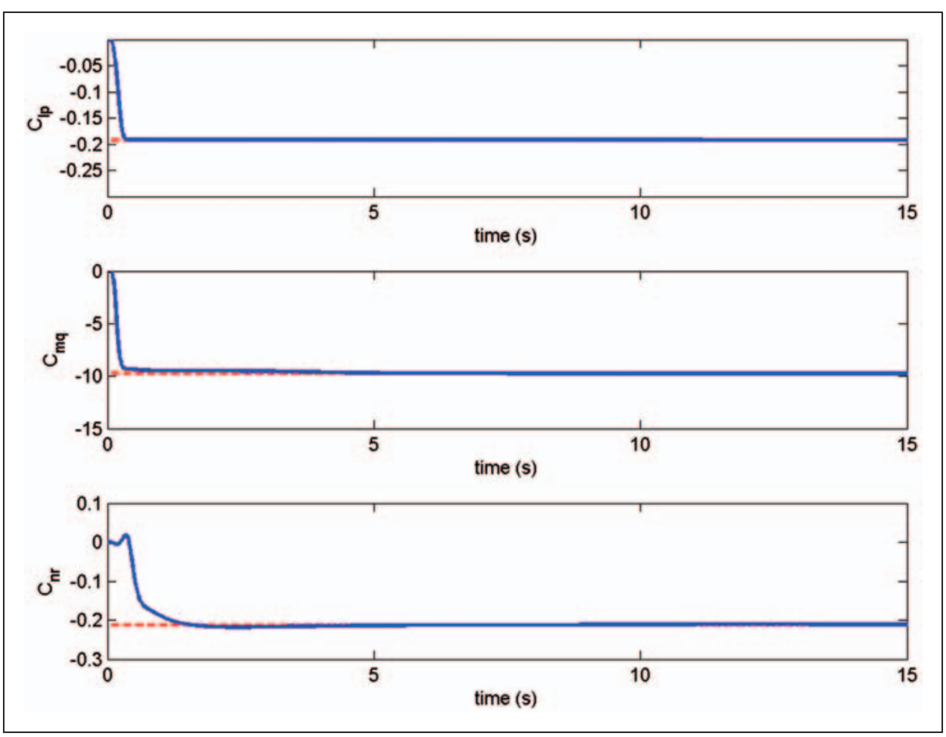

Figure 6. Time histories of the estimation for the aerodynamic moment coefficients.

The commands are shaped by the second-order linear command filters to generate the differentiable reference commands as follows

$$\frac{\alpha_d(s)}{\alpha_c(s)} = \frac{\omega_\alpha^2}{s^2 + 2\xi_\alpha\omega_\alpha + \omega_\alpha^2}$$
$$\frac{\beta_d(s)}{\beta_c(s)} = \frac{\omega_\beta^2}{s^2 + 2\xi_\beta\omega_\beta + \omega_\beta^2}$$
$$\frac{\phi_d(s)}{\phi_c(s)} = \frac{\omega_\phi^2}{s^2 + 2\xi_\phi\omega_\phi + \omega_\phi^2}$$

where

$$\omega_\alpha = \omega_\beta = \omega_\phi = 2\text{rad/s}$$
$$\xi_\alpha = \xi_\beta = \xi_\phi = 0.8$$

The adaptive flight control system is designed to track the smooth reference command. The final gains of the estimator are chosen as

$$\gamma_1 = 0 \quad \gamma_2 = 5 \quad \gamma_3 = 5$$
$$\gamma_1' = 10 \quad \gamma_2' = 10 \quad \gamma_3' = 10$$

The gains of the controller are

$$k_1 = 10 \quad k_2 = 5 \quad k_3 = 10$$
$$k_1' = 20 \quad k_2' = 10 \quad k_3' = 15$$

Figure 2 shows the command-tracking trajectory of the adaptive flight control system, where the dashed line corresponds to the reference trajectory and the solid line the response. During the simulation, the aircraft climbs up and down while simultaneously performing the banked turn. It is observed that the aircraft follows the desired trajectory with good tracking performance despite the fact that there are some unknown parameters. Figure 3 shows the control surface deflections needed in order to perform the maneuver, which are acceptable without the saturation. Figure 4 shows the time histories of angular rates during the maneuver; these angular rates are physical rational.

The convergence performance of the estimator for the unknown aerodynamic force coefficients can be seen in Figure 5. The true values are $C_{Y\beta} = -0.379$ and $C_{Z\alpha} = -3.25$. The time histories of the estimator for the unknown aerodynamic moment coefficients can be seen in Figure 6. The true values are $C_{lp} = -0.192$, $C_{nr} = -0.214$, and $C_{mq} = -9.83$. It can be observed that that estimates rapidly converge to their true values and are confined to true values after reaching them. The simulation results verify the estimation convergence performance of the estimator.

Conclusions

In this article, a general structure for the adaptive backstepping scheme based on invariant manifolds has been discussed. Based on this scheme, the flight control system for a small UAV is designed to track the command trajectory of the angle of attack, the sideslip angle, and the roll angle.

The adaptive control scheme consists of an estimator and a controller which are separately designed. The estimator which is used to estimate the unknown aerodynamic coefficients on-line relies on the notion of the invariance of the manifold. The estimator consists of a partial estimate generated by an update law and a non-linear function. The update law and non-linear function are selected so that the dynamics of the estimation error has a stable zero equilibrium, which also guarantees that the defined manifold is invariant. Once the estimate is confined to the manifold, it converges to its true value. The estimator can be exploited by combining it with the backstepping control law. The stability and convergence properties of the control law can be proved using the Lyapunov stability theory. The control law is derived by driving the Lyapunov function negative. This scheme is much easier to tune compared with the classical adaptive flight control law. Furthermore, this approach does not suffer from the undesired transient performance resulting from the unexpected dynamical behavior of parameter update laws.

The flight control system based on the proposed method is valid in the entire flight envelope and designed based on a primitive aerodynamic model, which would greatly improve the performance of the flight control system and reduce the cost of the flight control design. The numerical simulation demonstrates that the proposed adaptive flight control law can accomplish the satisfactory command tracking in spite of there being some unknown aerodynamic parameters.

Funding

This study was supported by Aeronautical Science Foundation of China (20100758002).

References

1. Blakelock JH. *Automatic control of aircraft and missiles*, 2nd ed. New York, NY: John Wiley, 1991.
2. Leith DJ and Leithead WE. Gain-scheduled control: relaxing slow variation requirements by velocity-based design. *AIAA J Guid Control Dyn* 2000; 23(6): 988–1000.

3. Wu S-L, Chen P-C, Chang K-Y, et al. Robust gain-scheduled control for vertical/short take-off and landing aircraft in hovering with time-varying mass and moment of inertia. *Proc IMechE, Part G: J Aerospace Engineering* 2008; 222(4): 473–482.
4. Kim S-H, Kim Y-S and Song C. A robust adaptive nonlinear control approach to missile autopilot design. *Control Eng Pract* 2004; 12(2): 149–154.
5. Snell SA, Enns DF and Garrard WL. Nonlinear inversion flight control for a supermaneuverable aircraft. *AIAA J Guid Control Dyn* 1992; 15(4): 976–984.
6. Bugajski DJ and Enns DF. Nonlinear control law with application to high angle-of-attack flight. *AIAA J Guid Control Dyn* 1992; 15(3): 761–767.
7. Reiner J, Balas GJ and Garrard WL. Flight control design using robust dynamic inversion and time-scale separation. *Automatica* 1996; 32(11): 1493–1504.
8. Khalil HK. *Nonlinear systems*, 3rd ed. Upper Saddle River, NJ: Prentice Hall, 2002.
9. Calise AJ, Hovakimyan N and Idan M. Adaptive output feedback control of nonlinear systems using neural networks. *Automatica* 2001; 37(8): 1201–1211.
10. Shin Y and Calise AJ. Adaptive control of advanced fighter aircraft in nonlinear flight regimes. *AIAA J Guid Control Dyn* 2008; 31(5): 1464–1477.
11. Lombaerts TJJ, Huisman HO, Chu QP, et al. Nonlinear reconfigurable flight control based on online physical model identification. *AIAA J Guid Control Dyn* 2009; 32(3): 727–748.
12. Shin DH and Kim Y. Reconfigurable flight control system design using adaptive neural networks. *IEEE Trans Control Syst Technol* 2004; 12(1): 87–100.
13. Ju H-S, Tsai C-C and Liu S-W. Design of longitudinal of axis full envelope control law by adaptive backstepping. In: *Proceedings of the 2004 lEEE international conference on networking, sensing and control*, Taipei, Taiwan, vol. 2, 21–24 March 2004. Piscataway: IEEE, pp.755–760.
14. Farrell J, Sharma M and Polycarpou M. Backstepping based flight control with adaptive function approximation. *AIAA J Guid Control Dyn* 2005; 28(6): 1089–1102.
15. Sonneveldt L, Chu QP and Mulder JA. Nonlinear flight control design using constrained adaptive backstepping. *AIAA J Guid Control Dyn* 2007; 30(2): 322–336.
16. Li CY, Jing WX and Gao CS. Adaptive backstepping-based flight control system using integral filters. *Aerosp Sci Technol* 2009; 13(2–3): 105–113.
17. Page AB and Steinberg ML. Effects of control allocation algorithms on a nonlinear adaptive design. In: *Proceedings of the AIAA guidance, navigation, and control conference and exhibit*, Portland, OR, 9–11 August 1999. Reston: AIAA, pp.1664–1674.
18. van Oort ER, Sonneveldt L, Chu QP and Mulder JA. A comparison of adaptive control designs for an over-actuator fighter aircraft model. In: *Proceedings of the AIAA guidance, navigation, and control conference and exhibit*, Honolulu, Hawaii, 18–21 August 2008. Reston: AIAA.
19. Astolfi A and Ortega R. Immersion and invariance: a new tool for stabilization and adaptive control of nonlinear systems. *IEEE Trans Autom Control* 2003; 48(4): 590–606.
20. Astolfi A, Karagiannis D and Ortega R. *Nonlinear and adaptive control with applications*. London: Springer-Verlag, 2008.
21. Karagiannis D and Astolfi A. Observer design for a class of nonlinear systems using dynamic scaling with application to adaptive control. In: *Proceedings of the 47th IEEE conference on decision and control*, Cancun, Mexico, 9–11 December 2008. Piscataway: IEEE, pp.2314–2319.
22. Byrnes CI, Priscoli FD and Isidori A. *Output regulation of uncertain nonlinear systems*. Boston, MA: Birkhuser, 1997.
23. Stephen W. *Introduction to applied nonlinear dynamical systems and chaos*, 2nd ed. New York, NY: Springer, 2003.
24. Karagiannis D and Astolfi A. Non-linear and adaptive flight control of autonomous aircraft using invariant manifolds. *Proc IMechE, Part G: J Aerospace Engineering* 2009; 224(4): 403–415.
25. Sonneveldt L, van Oort ER, Chu QP, et al. Immersion and invariance based nonlinear adaptive flight control. In: *Proceedings of the AIAA guidance, navigation, and control conference and exhibit*, Toronto, Ontario, 2–5 August 2010. Reston: AIAA.
26. Seo D and Akella MR. Non-certainty equivalent adaptive control for robot manipulator systems. *Syst Control Lett* 2009; 58(3): 304–308.
27. Lee KW and Singh SN. Immersion- and invariance-based adaptive control of a nonlinear aeroelastic system. *AIAA J Guid Control Dyn* 2009; 32(4): 1100–1110.
28. Lee KW and Singh SN. Noncertainty-equivalent adaptive missile control via immersion and invariance. *AIAA J Guid Control Dyn* 2010; 33(3): 655–665.
29. Ducard G and Geering HP. Efficient nonlinear actuator fault detection and isolation system for unmanned aerial vehicles. *AIAA J Guid Control Dyn* 2008; 31(1): 225–237.
30. Stevens BL and Lewis FL. *Aircraft control and simulation*, 2nd ed. New York, NY: John Wiley, 2003.
31. Ducard G, Geering HP and Dumitrescu E. Efficient control allocation for fault tolerant embedded systems on small autonomous aircrafts. In: *Proceedings of the IEEE international symposium on industrial embedded systems*, Antibes Juan-Les-Pins, 18–20 October 2006. Piscataway: IEEE, pp.1–10.
32. Lee T and Kim Y. Nonlinear adaptive flight control using backstepping and neural networks controller. *AIAA J Guid Control Dyn* 2001; 24(4): 675–682.
33. Bodson M. Evaluation of optimization methods for control allocation. *AIAA J Guid Control Dyn* 2002; 25(4): 703–711.
34. Ducard G and Geering HP. Airspeed control for unmanned aerial vehicles: a nonlinear dynamic inversion approach. In: *Proceeding of the IEEE 16th Mediterranean conference on control and automation*, Ajaccio, Corsica, France, 25–27 June 2008. Piscataway: IEEE, pp.676–681.